Pre-Steady-State Kinetics of the Microtubule·Kinesin ATPase†

Susan P. Gilbert and Kenneth A. Johnson*

Department of Biochemistry and Molecular Biology, 106 Althouse Laboratory, The Pennsylvania State University, University Park, Pennsylvania 16802

Received September 23, 1993; Revised Manuscript Received November 30, 1993®

ABSTRACT: The pre-steady-state kinetics of the microtubule·kinesin ATPase were investigated by chemical-quench flow methods using the *Drosophila* kinesin motor domain (K401) expressed in *Escherichia coli* [Gilbert, S. P., & Johnson, K. A. (1993) *Biochemistry 32,* 4677–4684]. The results define a minimal mechanism: $M{\cdot}K + ATP \overset{1}{\rightleftharpoons} (M){\cdot}K{\cdot}ATP \overset{2}{\rightleftharpoons} (M){\cdot}K{\cdot}ADP{\cdot}P_i \overset{3}{\rightleftharpoons} M{\cdot}K{\cdot}ADP + P_i \overset{4}{\rightleftharpoons} M{\cdot}K + ADP$, where M, K, and P_i represent microtubules, kinesin, and inorganic phosphate, respectively, with k_{+1} = 0.8–3 μM^{-1} s^{-1}, k_{-1} = 100–300 s^{-1}, k_{+2} = 70–120 s^{-1}, k_{+4} = 10–20 s^{-1}, and $k_{+3} \gg k_{-2}$ and $k_{+3} \gg k_{+4}$. Conditions were as follows: 25 °C, 20 mM HEPES, pH 7.2 with KOH, 5 mM magnesium acetate, 0.1 mM EDTA, 0.1 mM EGTA, 50 mM potassium acetate, 1 mM DTT. The experiments presented do not determine the step in the cycle where kinesin dissociates from the microtubule or the step at which kinesin reassociates with the microtubule; therefore, the steps that may represent kinesin as the free enzyme are indicated by (M). A burst of ADP product formation was observed during the first turnover of the enzyme in the acid-quench experiments that define the ATP hydrolysis transient. The observation of the burst demonstrates that product release is rate limiting even in the presence of saturating microtubule concentrations. The pulse–chase experiments define the time course of ATP binding to the microtubule·K401 complex. At low ATP concentrations, ATP binding limits the rate of the burst. However, at high concentrations of ATP, ATP binding is faster than the rate of ATP hydrolysis with k_{+2} = 70–120 s^{-1}. The amplitude of the burst of the ATP binding transient reached a maximum of 0.7 per site at saturating concentrations of ATP and microtubules. The amplitude of less than 1 is attributed to the fast k_{off} for ATP (k_{-1} = 100–300 s^{-1}) that leads to a partitioning of the M·K·ATP complex between ATP hydrolysis (k_{+2}) and ATP release (k_{-1}). These results indicate that ATP binds weakly to the M·K complex ($K^{app}_{d,ATP} \simeq 100\ \mu M$). ADP release ($k_{+4}$ = 10–20 s^{-1}) is rate limiting during steady-state turnover, indicating that microtubules activate the kinesin ATPase by increasing $k_{off,ADP}$ from 0.01 s^{-1} in the absence of microtubules to 10–20 s^{-1} at saturating microtubule concentrations.

Kinesin couples the energy of ATP hydrolysis to mechanical work to drive intracellular organelle movements along microtubules [reviewed by Vale (1987), Warner and McIntosh (1989), and Goldstein (1991)]. Since kinesin's discovery in 1985 (Vale *et al.,* 1985; Brady *et al.,* 1985; Scholey *et al.,* 1985), researchers have been intrigued by its motility characteristics and have attempted to understand the motility in the context of mechanistic information for the microtubule·axonemal dynein and actomyosin ATPases which have been studied extensively [reviewed by Johnson (1985), Eisenberg and Hill (1985), Hibberd and Trentham (1986), Goldman (1987), Geeves (1992), Taylor (1992), and Hackney (1992)]. However, the mechanistic experiments for the dynein and myosin ATPases used preparations from sources of protein involved in filament systems (axonemal dynein for ciliary beating; skeletal myosin and smooth muscle myosin for muscle contraction). In contrast, kinesin is a cytoplasmic motor which interacts with microtubules singly or as a small number of motors rather than as a part of a macromolecular assembly. Moreover, new molecular motors (kinesins, myosins, and dyneins) are still being discovered (Endow & Titus, 1992; Goodson & Spudich, 1993; Skoufias & Scholey; 1993). Because these motors show a number of structural and functional properties in common, it is now possible to determine if there is a common kinetic pathway for all contractile systems or if there are unique mechanisms for the different motors. As we study these newly discovered motors in detail, the results should provide information to understand the common mechanistic features that are required to couple nucleotide hydrolysis to force production to begin to define the variations that result in the functional and motility differences observed.

Kinesin is the first of the cytoplasmic motors to be investigated using pre-steady-state kinetic techniques (Hackney, 1988; Hackney *et al.,* 1989; Sadhu & Taylor, 1992). The initial kinesin mechanistic experiments have focused on the native bovine brain kinesin preparation studied in the absence of microtubules. Hackney *et al.* (1988, 1989) demonstrated that ADP is tightly bound such that kinesin when purified contains a stoichiometric amount of ADP bound at the active site. Furthermore, it is ADP release rather than phosphate release that is rate limiting during steady-state turnover, and the rate of ADP release is increased by the addition of microtubules. The nucleotide-free kinesin also exhibits a burst of product formation. This result indicates that ATP binding and hydrolysis occur at fast rates to produce ADP and P_i at the active site, and slow product release limits the steady-state rate in the absence of microtubules (Hackney *et al.,* 1989; Sadhu & Taylor, 1992). These results established the basic characteristics of the kinesin mechanism which is similar to both myosin and dynein. For both myosin and dynein as free enzymes in solution, a burst of product formation was observed which indicates that the rates of ATP binding and

† This research was supported by grants to K.A.J. (GM26726 from the National Institutes of Health) and S.P.G. (postdoctoral fellowship from the Muscular Dystrophy Association).

* To whom correspondence should be addressed. Telephone: 814-865-1200. FAX: 814-865-3030.

® Abstract published in *Advance ACS Abstracts,* February 1, 1994.

0006-2960/94/0433-1951$04.50/0

hydrolysis are faster than the steady state rate of product release (Lymn & Taylor, 1970, 1971; Johnson, 1983). Furthermore, for both myosin and dynein, P_i release occurs prior to ADP release from the active site (Trentham *et al.*, 1972; Holzbaur & Johnson, 1989a). For actomyosin, F-actin increases the rate of both P_i and ADP release (Lynn & Taylor, 1971). In contrast, microtubules activate the rate of ADP release from dynein which is rate limiting during steady-state turnover, but microtubules do not alter the rate of phosphate release (Holzbaur & Johnson, 1989a,b). Microtubules rebind to the dynein·ADP intermediate. In the case of myosin, it is the myosin·ADP·P_i species that rebinds to F-actin (Sleep & Boyer, 1978; Sleep & Hutton, 1980; Hackney & Clark, 1984). Kinesin is unique in its very tight binding of ADP to the active site. The observation that kinesin is purified with ADP bound indicates that K·ADP is an important intermediate in the pathway and suggests that K·ADP is the predominant species that rebinds to the microtubules.

Sadhu and Taylor's experiments (1992) at higher protein concentrations extended the initial pre-steady-state results of the kinesin pathway in the absence of microtubules. The rates of the nucleotide-binding steps were determined by fluorescence changes that occur upon the binding of the nucleotide analogs, mant-ATP and mant-ADP.[1] The results demonstrated that the binding of both mant-ATP and mant-ADP occurs by the formation of an initial collision complex that is in rapid equilibrium with the free nucleotide followed by a conformational change in the protein. Substrate binding for both myosin and actomyosin also occurs by a rapid equilibrium followed by a change in conformation. For actomyosin, the change in conformation was correlated with the dissociation of the myosin·ATP complex from F-actin (Lymn & Taylor, 1971). Although the experiments using mant-ATP and mant-ADP were not done for axonemal dynein, a similar sequence of steps for nucleotide binding could be expected.

The initial mechanistic studies with native kinesin have been critical in defining the basic characteristics of kinesin as an ATPase and the determination of a minimal mechanism of the free enzyme in the absence of microtubules. However, the pre-steady-state kinetic analysis has been limited by the native bovine kinesin preparation. The bovine brain kinesin preparations are heterogeneous in light chain content (Hackney *et al.*, 1989; Sadhu & Taylor, 1992) and possibly in kinesin-like isoforms (Stewart *et al.*, 1991; Aizawa *et al.*, 1992; Gho *et al.*, 1992). Furthermore, the presence of a subpopulation of kinesin molecules that are in the folded 9 S conformation may contribute to the biphasic kinetics and low steady-state turnover rate observed in the presence of microtubules (Hackney *et al.*, 1991, 1992). Lastly, many of the experiments needed to define the mechanism accurately cannot be done because of the low amounts of kinesin protein purified from bovine brain.

For our mechanistic and structural studies on the kinesin ATPase, we have focused our efforts to develop a bacterially expressed preparation of active kinesin motor domains (Gilbert & Johnson, 1993). The truncated protein (designated K401) contains the N-terminal 401 amino acids of the *Drosophila melanogaster* kinesin heavy chain and is purified from *Escherichia coli* as an over-expressed protein. K401 is a homogeneous preparation purified in milligram amounts. The preliminary kinetic characterization indicates that K401 is fully active and demonstrates the kinetic properties expected of a native kinesin. K401 has very low ATPase activity in the absence of microtubules (k_{cat} = 0.01 s^{-1}) which is stimulated ~1000-fold at saturating concentrations of microtubules and MgATP (k_{cat} = 10 s^{-1}; $K_{0.5,MT}$ = 0.9 μM tubulin; $K_{m,ATP}$ = 31 μM). Like native kinesin, K401 when purified contains ADP tightly bound at its active site, and the release of ADP from the active site occurs at a rate equal to steady-state turnover ($k_{cat} \simeq$ 0.01 s^{-1}). Active-site titrations indicate that there is one ATPase site per K401 molecule and that K401 binds to microtubules with an axial periodicity of 8 mm, *i.e.*, a stoichiometry of one kinesin motor domain per tubulin dimer (Harrison *et al.*, 1993).

In the experiments presented here, we examine the pre-steady-state kinetics of the microtubule·kinesin ATPase pathway using the MT·K401 complex and chemical quench flow techniques to measure the steps of ATP binding, ATP hydrolysis, and ADP release during the firsr turnover of the enzyme.

EXPERIMENTAL PROCEDURES

Materials. [α-^{32}P]ATP (>3000 Ci/mmol) was purchased from ICN Biomedicals and PEI cellulose F TLC plates (EM Separations of E. Merck, 20 × 20 cm, plastic backed) from Curtin Matheson Scientific, Inc. Taxol was the generous gift of the Drug Synthesis and Chemistry Branch, Division of Cancer Treatment, National Cancer Institute.

Media and Buffers. The following buffers were used for the experiments described: ATPase buffer (20 mM HEPES, pH 7.2 with KOH, 5 mM magnesium acetate, 0.1 mM EDTA, 0.1 mM EGTA, 50 mM potassium acetate, 1 mM DTT); PM buffer (100 mM PIPES, pH 6.7 with KOH, 5 mM magnesium acetate, 1 mM EGTA).

Protein Purification. Procedures for the expression and purification of the *Drosophila* kinesin motor domain, K401, have been described previously (Gilbert & Johnson, 1993). The protein concentration of K401 was determined spectrophotometrically using the extinction coefficient 29340 M^{-1} cm^{-1} for K401 containing 1 ADP bound per K401. K401 represents 91% of the absorbance at 280 nm (Gilbert & Johnson, 1993). Each preparation of K401 was evaluated by active-site titration as well as steady-state ATPase assays to determine the k_{cat} in the absence of microtubules and the k_{cat} at saturating concentrations of microtubules and MgATP (Gilbert & Johnson, 1993). For the experiments reported, seven preparations of K401 were used. The active-site titration (based upon stoichiometry of binding of [α-^{32}P]ADP in a nitrocellulose binding assay) for each K401 preparation indicated that the concentration of active sites was equal to the K401 concentration based on protein determinations. There was some variability between K401 preparations in the steady-state k_{cat} at saturating concentrations of microtubules and MgATP as well as some variability in the elementary rate constants. All experiments reported were performed with at least three different K401 preparations, and the errors in the rates reported include the variability seen in different preparations.

Bovine brain microtubules were prepared by two cycles of temperature-dependent polymerization and depolymerization (Shelanski *et al.*, 1973; Sloboda *et al.*, 1976), and tubulin was separated from microtubule-associated proteins by the method

[1] The abbreviations used are as follows: DTT, dithiothreitol; EGTA, ethylene glycol bis(2-aminoethyl ether)-*N,N,N',N'*-tetraacetic acid; HEPES, 4-(2-hydroxyethyl)-1-piperazineethanesulfonic acid; mant-ADP, 2'(3')-*O*-(*N*-methylanthraniloyl)-ADP; mant-ATP, 2'(3')-*O*-(*N*-methylanthraniloyl)-ATP; MT·dynein, microtubule-dynein; MT·K401, microtubule·K401; PEI, poly(ethylenimine); PIPES, piperazine-*N,N'*-bis(ethanesulfonic acid); SDS–PAGE, sodium dodecyl sulfate–polyacrylamide gel electrophoresis; TLC, thin-layer chromatography.

of Borisy *et al.* (1974) as modified by Omoto and Johnson (1986). On the morning of each experiment, an aliquot of tubulin was thawed, diluted with PM buffer to 10–15 mg/mL of protein, adjusted to 1 mM MgGTP, and cold depolymerized for 30 min on ice. The tubulin was then centrifuged (microfuge, 14 000 rpm, 15 min, 4 °C) to sediment aggregates of tubulin. The supernatant with soluble tubulin was adjusted to 20 μM taxol followed by incubation at 34 °C for 20 min to polymerize the microtubules. The microtubule preparation was diluted in PM buffer plus 20 μM taxol to dilute the GTP concentration to 0.1 mM and stabilize the microtubules. The preparation was incubated for an additional 20 min at 34 °C followed by centrifugation (Sorvall SS34 rotor, 18 000 rpm, 20 min, 4 °C). The microtubule pellet was resuspended in ATPase buffer plus 20 μM taxol, and the protein concentration was determined by the Schacterle and Pollack (1973) modification of Lowry *et al.* (1951).

For the ATPase assays, the MT·K401 complex in ATPase buffer plus 20 μM taxol was incubated for 10 min. The experiments described below (see Figures 1 and 2) verified that ADP was displaced from the active site of K401 in the presence of excess microtubules.

Rapid Quench Experiments. The ATPase assays were performed at 25 °C in ATPase buffer using a chemical quench flow instrument designed by Johnson (1986) and built by KinTek Instruments (University Park, PA). For each time point, the preformed MT·K401 complex was loaded into one loop (15 μL), and the substrate [α-^{32}P]ATP in ATPase buffer was loaded into the second loop (15 μL) of tubing. A computer-controlled stepper motor drives the syringes which forces the two reactants together and through the delay line. In the delay line the reaction mixture is incubated for the designated time of the reaction which varied from 3 ms to 4 s. The reaction mixture was quenched with 80 μL of 2 N HCl and expelled from the instrument. Chloroform (100 μL) was added immediately to the reaction mixture to denature the protein, followed by neutralization by the addition of 21 μL of 2 M Tris–3 M NaOH. These acid-quench experiments determined the time course of ATP hydrolysis (the formation of acid-labile products ADP and P_i); therefore, the product formed for each time point represents the sum of K·[α-^{32}P]ADP·P_i intermediate, K·[α-^{32}P]ADP intermediate, and [α-^{32}P]ADP released from the active site.

Pulse–Chase Experiments. The time course of ATP binding was measured by chasing with a minimum of 10–100-fold excess unlabeled MgATP (5 mM final concentration for most experiments in ATPase buffer plus 5 μM taxol) for 0.7 s (10 half-lives of enzyme turnover, k_{cat} = 10 s^{-1}). For these experiments, the reaction mixture is incubated in the delay line for the specified time (4 ms to 4 s) as in the acid-quench experiments. However, the unlabeled MgATP was in the quench syringe rather than HCl; thus, the binding of [α-^{32}P]-ATP was followed by the addition of a large excess of MgATP rather than terminated by the addition of acid. A modification was made in the quench–flow instrument to introduce an additional delay after the addition of the MgATP quench so that the quenched reaction was held in the exit line the 0.7 s for the MgATP chase. The reaction mixture was then expelled from the instrument directly into 100 μL of 2 N HCl to terminate the reaction, followed by the addition of chloroform (100 μL) to denature the protein, and 43 μL of 2 M Tris–3 M NaOH to neutralize the pH. In the pulse–chase experiments, bound [α-^{32}P]ATP would be converted to [α-^{32}P]ADP + P_i, yet any substrate unbound or bound loosely to the active site would be diluted by the excess unlabeled MgATP. This pulse–chase experiment measures the time course of the formation of a kinetically stable kinesin·ATP complex preceding ATP hydrolysis. This method however detects only the fraction of enzyme–substrate complex that proceeds in the forward direction and defined by the ratio

Scheme 1

$$M{\cdot}K + ATP \underset{k_{-1}}{\overset{k_{+1}}{\rightleftharpoons}} (M){\cdot}K{\cdot}ATP \underset{k_{-2}}{\overset{k_{+2}}{\rightleftharpoons}} (M){\cdot}K{\cdot}ADP{\cdot}P_i \underset{k_{-3}}{\overset{k_{+3}}{\rightleftharpoons}}$$

$$M{\cdot}K{\cdot}ADP + P_i \underset{k_{-4}}{\overset{k_{+4}}{\rightleftharpoons}} M{\cdot}K + ADP$$

$$k_{+2}/(k_{+2} + k_{-1})$$

Figure 4 shows the pulse–chase experimental results as a function of ATP concentration. For the 600 μM [α-^{32}P]-MgATP experiment (□), the 5 mM MgATP chase concentration was not sufficiently high to maintain an adequate ATP dilution during the chase time based on the following calculation of product formation:

[K401 during chase](0.7-s chase time)(k_{cat}) × (ATP dilution during chase)

Therefore, each data point for the 600 μM [α-^{32}P]ATP transient in Figure 4 was adjusted for the 3 μM ADP that would form during the chase period due to insufficient dilution of the radiolabeled ATP. The 5 mM chase required no correction at lower [α-^{32}P]ATP concentrations.

The concentrations for K401, microtubules (tubulin), taxol, MgADP, and MgATP reported in the paper are the final concentrations after the enzyme and substrate are mixed as described for the rapid quench protocol.

Product Analysis. [α-^{32}P]ADP and P_i were separated from [α-^{32}P]ATP by PEI–cellulose TLC plates (eluted with 0.6 M potassium phosphate buffer, pH 3.4), and the radiolabeled ADP and ATP were quantitated using a Betascope 603 blot analyzer (Betagen, Waltham, MA).

Data Analysis. The kinetic data were modeled using the KINSIM kinetic simulation program provided by Drs. Carl Frieden and Bruce Barshop, Washington University, St. Louis, MO (Barshop *et al.*, 1983) as modified by Anderson *et al.* (1988). All curves were fit to the single mechanism in Scheme 1 with the rate constants shown in Table 1. The acid-quench transients were modeled by acid output = K·ADP·P_i + ADP. However, for the pulse–chase experiments, the partitioning that occurred at the K·ATP intermediate must be considered. For these transients

$$\text{chase output} = X1 * K{\cdot}ATP + K{\cdot}ADP{\cdot}P_i + ADP$$

The partitioning factor, X1, is the fraction of the K·ATP intermediate that proceeds toward hydrolysis with

$$X1 = k_{+2}/(k_{+2} + k_{-1})$$

Numerical integration using the KINSIM program was used by an iterative process, varying one rate constant at a time. The ranges to each rate constant were assigned on the basis of the following criteria. The mechanism (Scheme 1) with rate constants fit the data of all experiments, and the rate constants satisfied the equations

$$k_{cat} = k_{+2}k_{+4}/(k_{+2} + k_{-2} + k_{+4}) \quad (1)$$

Table 1: Microtubule·Kinesin Kinetic Constants[a]

reaction	k_+	k_-	K_{eq}
M·K + ATP ⇌ (M)·K·ATP	0.8–3 μM^{-1} s^{-1}	100–300 s^{-1}	0.01 μM^{-1}
(M)·K·ATP ⇌ (M)·K·ADP·P_i	70–120 s^{-1}		
(M)·K·ADP·P_i ⇌ (M)·K·ADP + P_i	fast[b]		
M·K·ADP ⇌ M·K + ADP	10–20 s^{-1}		
K + ATP ⇌ K·ATP			
K·ATP ⇌ K·ADP·P_i			
K·ADP·P_i ⇌ K·ADP + P_i	fast[b]		
K·ADP ⇌ K + ADP	0.01 s^{-1}[c]		
k_{cat} for M·K	10–20 s^{-1}		
k_{cat} for K	0.01 s^{-1} [c]		

[a] These kinetic constants represent the best global fit for all the steady-state and pre-steady-state kinetic data presented in this paper. The equilibrium constant for ATP binding was calculated for the forward reaction as written. Conditions were as follows: 20 mM HEPES, pH 7.2 with KOH, 5 mM magnesium acetate, 0.1 mM EDTA, 0.1 mM EGTA, 50 mM potassium acetate, 1 mM DTT at 25 °C. [b] Hackney, 1988. [c] Gilbert & Johnson, 1993.

$$K_d = k_{-1}/k_{+1} \quad (2)$$

The data presented in Figures 4 and 5, parts B and C, were obtained from the fits of the pre-steady-state data to the biphasic burst equation

$$\text{product} = A[1 - \exp(-k_b t)] + k_{ss} t \quad (3)$$

where A is the amplitude of the burst; k_b, the rate of the presteady state burst phase; k_{ss}, the rate of the linear phase which corresponds to steady-state turnover; and t, the time in milliseconds. The data in Figures 4B and 5B were fit to the equation

$$k_{burst} = \frac{A_{max}[\text{MgATP}]}{(K^{app}_{d,ATP} + [\text{MgATP}])} + k_{off,ATP} \quad (4)$$

where k_{burst} is the first-order rate constant of the pre-steady-state exponential phase and A_{max} is the maximum burst amplitude. The initial linear phase of the hyperbola predicts the apparent second-order rate constant for ATP binding, k_{+1}. The data in Figures 4C and 5C were fit to a hyperbola

$$A = \frac{A_{max}[\text{MgATP}]}{(K^{app}_{d,ATP} + [\text{MgATP}])} \quad (5)$$

where A is the amplitude of the burst and A_{max} is maximum burst amplitude.

The data were fit to eqs 3–5 by nonlinear regression using KaleidaGraph Software (Synergy Software, Reading, PA).

RESULTS

Burst of Product Formation. We began the pre-steady-state analysis of the MT·K401 ATPase by a series of rapid quench experiments to examine the kinetics of the first and subsequent turnovers of the enzyme. The MT·K401 complex was preformed with 10 μM K401 and microtubules (36 μM tubulin) in excess and at a microtubule concentration shown previously to activate maximally the steady-state ATPase activity of K401 (Gilbert & Johnson, 1993). The final concentration after mixing in the rapid quench was 5 μM K401 and 18 μM microtubules. Figure 1 shows the time course for the pulse–chase and acid-quench experiments at three concentrations of [α-^{32}P]MgATP. The data indicate

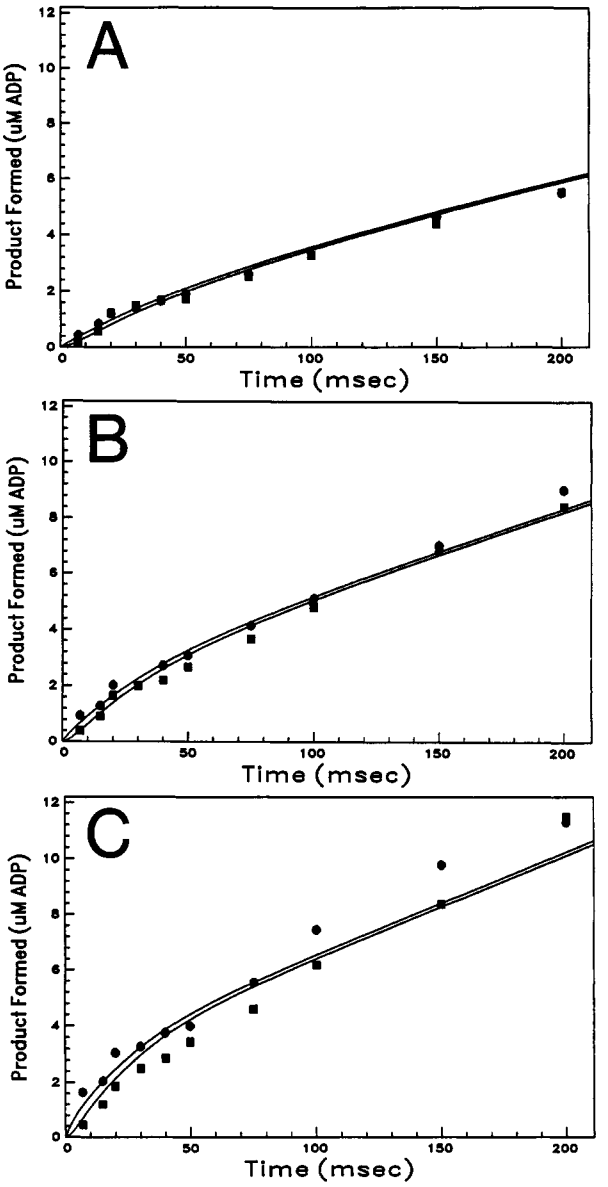

FIGURE 1: Pre-steady-state kinetics of ATP binding and hydrolysis at 18 μM tubulin. The ATPase assays were carried out at 25 °C according to the rapid-quenching protocol, and each reaction mixture contained the MT·K401 complex with microtubules at 18 μM tubulin and 5 μM K401. All concentrations reported represent final concentrations after mixing 1:1 in the rapid quench instrument. The time courses of ATP binding (●) and ATP hydrolysis (■) were determined for three different [α-^{32}P]MgATP concentrations (A, 25 μM; B, 50 μM; C, 100 μM). The curves were calculated by numerical integration according to the mechanism in Scheme 1 with the following rate constants: k_{+1} = 1.8 μM^{-1} s^{-1}, k_{-1} = 200 s^{-1}, k_{+2} = 75 s^{-1}, k_{+4} = 10 s^{-1}.

that the kinetics of ATP binding (pulse–chase experimental design) were very similar to the kinetics for ATP hydrolysis (acid-quench) at the [α-^{32}P]MgATP concentrations examined. Furthermore, the kinetics for both the ATP binding and ATP hydrolysis transients were biphasic. There was an initial fast rate of ADP·P_i formation (the burst) that corresponds to the first turnover, followed by a slower rate of product formation (the linear phase) that corresponds to steady-state turnover. The burst rate at ~65 s^{-1} (exponential phase) for 100 μM [α-^{32}P]MgATP was faster than subsequent turnovers at 9 s^{-1} (linear phase), and the rate of the linear phase is in good agreement with the k_{cat} at 10 s^{-1} determined by steady-state rate measurements for this K401 preparation. The observation of a pre-steady-state burst in the acid quench experiments is

indicative that the rate-limiting step of the MT·K401 pathway during steady-state turnover occurs after ATP hydrolysis.

In the pre-steady-state experiments presented in Figure 1, the amplitude of the initial burst of ADP·P_i formation is proportional to the concentration of active K401. In the acid-quench experiments, the burst amplitude is less than or equal to the concentration of the K·ADP·P_i intermediate. During the time of the chase in the pulse–chase experiments, the [α-^{32}P]ATP bound at the active site is converted to [α-^{32}P]-ADP + P_i. [α-^{32}P]ATP unbound or bound loosely to the active site is diluted by the excess unlabeled MgATP. Therefore, the pulse–chase experiment detects the fraction of K·[α-^{32}P]ATP complex that partitions in the forward direction as defined by the ratio $k_{+2}/(k_{+2} + k_{-1})$. Because the burst amplitude for the pulse–chase experiments is the sum of the K·[α-^{32}P]ATP that partitions in the forward direction and the products already formed at the active site, we anticipated a burst amplitude for these experiments to be equal to the K401 concentration used in the experiment (5 μM). Yet, even at 100 μM [α-^{32}P]MgATP, the burst amplitude was significantly less than 5 μM. A burst amplitude that is less than the enzyme concentration in the pulse–chase experiments could result for the following reasons: (1) inactive enzyme, (2) K401 with ADP bound at the active site, (3) microtubule bundling, (4) ATP concentration not high enough to saturate enzyme-active sites, (5) fast dissociation of ATP from kinesin (k_{-1}). Each of these hypotheses was evaluated experimentally, and the results are presented below.

Active-Site Concentration. A common cause of a reduced burst amplitude is inactive enzyme or fewer active sites than anticipated by protein determinations. Yet, the active-site titrations based upon the binding of [α-^{32}P]ADP in the absence of microtubules indicated that this preparation of K401 was 100% active.

MT·K·ADP. For the initial rapid quench experiments, the MT·K401 complex was preformed with K401 as purified, *i.e.*, with ADP bound at the active site. It was assumed that at saturating microtubule concentrations, ADP release from K401 would be rapid and that ADP would remain in solution rather than rebinding to the MT·K401 complex. This assumption was based on the steady-state k_{cat} of 10 s^{-1} (Gilbert & Johnson, 1993). However, if the MT·K401 complex were in equilibrium with MT·K401·ADP, kinetics such as those observed in Figure 1 with a reduced burst amplitude might be expected. The experiment presented in Figure 2 tests directly the assumption that microtubules would rapidly stimulate ADP release from the active site of K401 and that the ADP in solution would not inhibit the pre-steady-state burst kinetics. This experiment was similar to the 50 μM [α-^{32}P]MgATP pulse–chase experiment in Figure 1B except 20 μM MgADP was also added to the reaction mixture. Figure 2 shows the results with (1) 20 μM MgADP added to the [α-^{32}]ATP syringe, (2) 20 μM MgADP preincubated with K401 and microtubules during formation of the MT·K401 complex, and (3) no additional MgADP added to the reaction mixture. It was anticipated that if the 5 μM ADP initially bound at the active site of K401 were leading to an equilibrium of MT·K401 complexes (MT·K401 $\rightleftarrows$ MT·K401·ADP), then the addition of 20 μM MgADP should shift the equilibrium toward MT·K401·ADP. Experimentally, one would observe a further reduction of the burst amplitude or a reduction in the rate of the burst. The results in Figure 2 clearly show that there is no significant difference in the kinetic data either in the presence or absence of added MgADP. Furthermore, these results suggest that ADP even as high as 25 μM is not

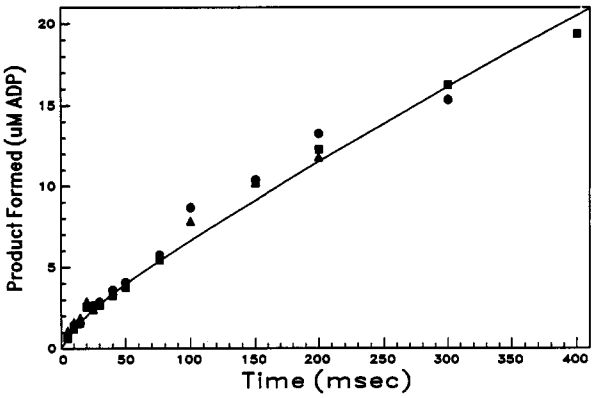

FIGURE 2: Pre-steady-state kinetics of ATP binding in the presence and absence of added ADP. The MT·K401 complex (5 μM K401 with microtubules at 18 μM tubulin) was preformed and reacted with 50 μM [α-^{32}P]MgATP in the absence of added MgADP (●), in the presence of 20 μM MgADP added to [α-^{32}P]ATP syringe (■), and in the presence of 20 μM MgADP preincubated with the MT·K401 complex (▲). The curve was calculated by numerical integration according to the mechanism in Scheme 1 with the following rate constants: k_{+1} = 1.8 μM^{-1} s^{-1}, k_{-1} = 200 s^{-1}, k_{+2} = 100 s^{-1}, k_{+4} = 20 s^{-1}.

inhibiting the MT·K401 ATPase; thus, the apparent K_I for ADP must be significantly higher than 25 μM in the presence of 50 μM ATP.

Microtubule Concentration. The initial burst experiments were designed with microtubules in excess. However, Harrison *et al.* (1993) demonstrated that K401 binds microtubules at saturation with a stoichiometry of 1 K401 per tubulin dimer. We tested the hypothesis that excess microtubules were resulting in microtubule bundling promoted by a second, nonnucleotide-dependent microtubule binding site on K401. If this bundling were to occur, it could result in the reduced burst amplitude and pre-steady-state kinetics observed, for example by a conformational change in K401 or by local concentration effects. Figure 3 shows the results from both pulse–chase and acid-quench experiments in which the MT·K401 complex was preformed with microtubules and K401 at a 1:1 ratio and at two substrate concentrations (50 and 100 μM [α-^{32}P]MgATP). The pre-steady-state kinetics for the ATP binding and the ATP hydrolysis transients at both [α-^{32}P]MgATP concentrations are in good agreement with the results with microtubules in excess (Figure 1, parts B and C). The curves in both Figures 1 and 3 were simulated to the mechanism in Scheme 1 with the same rate constants.

The results presented in Figures 2 and 3 evaluated the obvious technical reasons for the reduced burst amplitude and the pre-steady-state kinetics observed. To explore mechanistic reasons for the observed burst kinetics, a series of pulse–chase and acid-quench experiments was performed at increasing concentrations of [α-^{32}P]MgATP attempting to saturate the rate of substrate binding such that the chemistry step (ATP hydrolysis) limits the rate of the burst.

Time Course of ATP Binding. Pulse–chase experiments for the MT·K401 complex were performed at increasing concentrations of [α-^{32}P]MgATP to obtain information about the equilibrium constant for ATP binding to the MT·K401 complex. Figure 4A shows the results of product formation as a function of time, and the curves were obtained from the computer simulations of the data to the mechanism in Scheme 1 with the rate constants presented in the figure legend. These data reveal that the first-order burst rates increase with increasing concentrations of [α-^{32}P]MgATP; therefore, the rate of ATP binding to the MT·K401 complex increases with

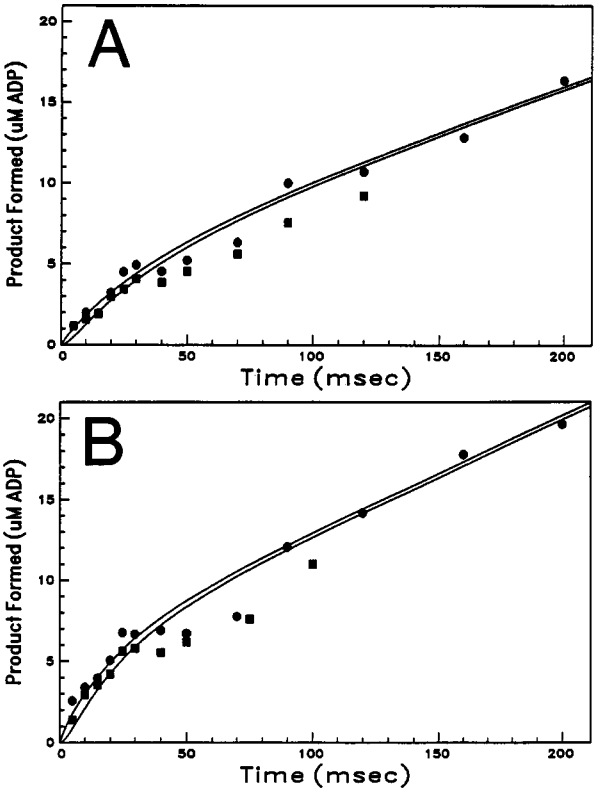

FIGURE 3: Pre-steady-state kinetics of ATP binding and hydrolysis with microtubules and K401 at 1:1. The MT·K401 complex (10 μM K401 with microtubules in slight excess at 12 μM tubulin) was preformed and reacted with [α-^{32}P]MgATP at 50 μM (A) and 100 μM (B). The time courses of ATP binding (●) and ATP hydrolysis (■) are shown. The curves were calculated by numerical integration according to the mechanism in Scheme 1 with k_{+1} = 1.8 μM^{-1} s^{-1}, k_{-1} = 200 s^{-1}, k_{+2} = 75 s^{-1}, k_{+4} = 10 s^{-1}.

increasing concentrations of MgATP. The data for each transient in Figure 4A were also fit to the pre-steady-state burst equation (eq 3). The rate constants and amplitudes obtained from the burst equation were plotted in Figure 4, parts B and C. The dependence of the burst rate on the [α-^{32}P]-MgATP concentration is shown in Figure 4B, and the data indicate that the first-order rate of the burst is saturating with a maximum burst rate of 239 ± 66 s^{-1}. The observation that the burst rate in the pulse–chase experiments saturates at increasing concentrations of substrate would indicate that there is a rate-limiting conformational change that occurs prior to the chemical step (k_{+2}) on the order of 170–300 s^{-1} (addressed in the Discussion section). The result in Figure 4B that the burst rate saturates with increasing concentrations of ATP is inconsistent with the minimal mechanism proposed in Scheme 1 and the time courses in Figure 4A. The observation of saturation in Figure 4B may be due to a mechanism more complex than one-step binding. Alternatively, the data for the first-order rate constants for the burst obtained from the burst equation (eq 3) have large standard errors because of the weak binding of ATP to the MT·K401 complex. As the burst rate increases with increasing concentrations of ATP, the fast rates become more difficult to measure accurately with a maximum measurable burst rate for the MT·K401 system on the order of 300–400 s^{-1}. Because of the technical problems associated with obtaining these burst rates, the interpretation of the results in Figure 4B must be considered carefully (see the Discussion section also).

The initial slope in Figure 4B defines the apparent second-order rate constant for ATP binding (k_{+1}) to be 1 μM^{-1} s^{-1}.

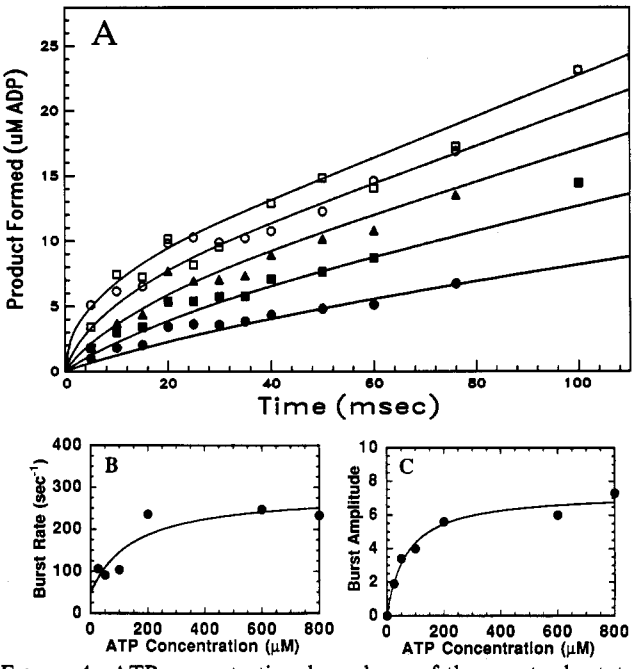

FIGURE 4: ATP concentration dependence of the pre-steady-state kinetics of ATP binding. The MT·K401 complex (10 μM K401 with microtubules in slight excess at 12 μM tubulin) was preformed and allowed to react with [α-^{32}P]MgATP for 5–200 ms, followed by the 5 mM MgATP chase as described in Experimental Procedures. Panel A shows the transients for each [α-^{32}P]ATP concentration: 25 μM (●), 50 μM (■), 100 μM (▲), 200 μM (○), and 600 μM (□). The curves were calculated by numerical integration according to the mechanism in Scheme 1 with the following rate constants: k_{+1} = 1.8 μM^{-1} s^{-1}, k_{-1} = 200 s^{-1}, k_{+2} = 100 s^{-1}, k_{+4} = 20 s^{-1}. Panel B, the pre-steady-state burst rate determined for each transient using the burst equation (eq 3) and plotted as a function of [α-^{32}P]ATP concentration. These data were fit to eq 4 (solid line). The initial linear part of the fit predicts the apparent second-order rate constant for ATP binding (k_{+1}) to be 1 μM^{-1} s^{-1}, the maximum burst rate = 239 ± 66 s^{-1}, and k_{-1} = 49 ± 78 s^{-1}. Panel C, the amplitude of the pre-steady-state burst determined for each transient using eq 3 and plotted as a function of [α-^{32}P]MgATP concentration. The data were fit to a hyperbola (solid line) with the maximum burst amplitude = 7.3 ± 0.4 μM and $K_{d,ATP}^{app}$ = 69 ± 14 μM. Panels B and C include additional data obtained from experiments not shown in panel A.

The burst amplitude is shown as a function of substrate concentration in Figure 4C; the data were fit to a hyperbola with the maximum burst amplitude at 7.3 ± 0.4 μM and $K_{d,ATP}^{app}$ = 69 ± 14 μM.

The ATP concentration dependence of the pre-steady-state kinetics in these pulse–chase experiments clearly shows that even at very high ATP concentrations, the amplitude of the burst is less than 1 per active site. We attribute the reduced burst amplitude to a fast off rate for ATP (k_{-1} = 100–300 s^{-1}). Experiments to measure directly k_{-1} were not possible. The determination of k_{-1} reported here was made from the computer simulations to the mechanism in Scheme 1 with the rate constants in the figure legends of Figures 4A and 5A. Further experimental support of this fast $k_{off,ATP}$ is the $K_{d,ATP}^{app}$ determined from the data in Figures 4C and 5C. The true dissociation constant for ATP binding is defined by eq 2:

$$K_d = k_{-1}/k_{+1} \quad (2)$$

therefore, the ratio of k_{-1}/k_{+1} must be consistent with the $K_{d,ATP}^{app}$ determined in Figures 4C and 5C. The K_d calculated from the rate constants, k_{-1} and k_{+1}, is ~100 μM. The $K_{d,ATP}^{app}$ determined from Figure 4C is 69 ± 14 μM, and from

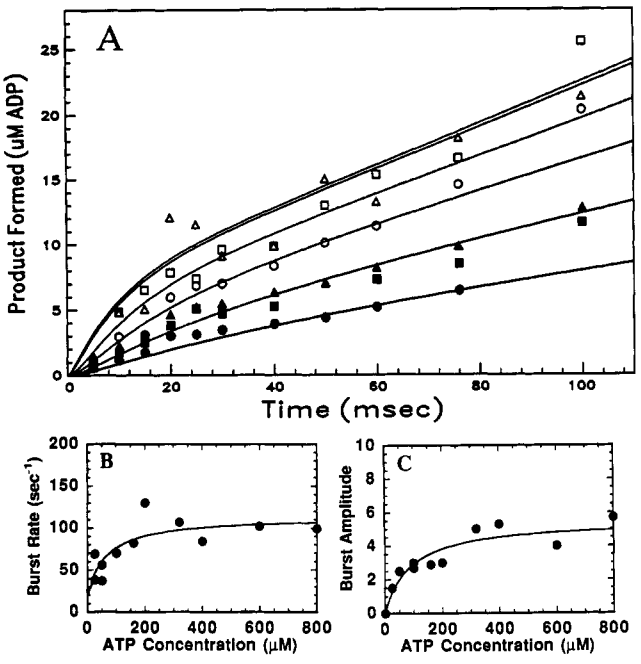

FIGURE 5: ATP concentration dependence of the pre-steady-state kinetics of ATP hydrolysis. The MT·K401 complex (10 μM K401 with microtubules in slight excess at 12 μM tubulin) was preformed and reacted with [α-^{32}P]MgATP for 5–200 ms, followed by the acid quench as described in Experimental Procedures. Panel A shows the transients for each [α-^{32}P]MgATP concentration: 25 μM (●), 50 μM (■), 100 μM (▲), 200 μM (○), 600 μM (□), and 800 μM (△). The curves were calculated by numerical integration according to the mechanism in Scheme 1 with the following rate constants: k_{+1} = 1.8 μM^{-1} s^{-1}, k_{-1} = 200 s^{-1}, k_{+2} = 100 s^{-1}, k_{+4} = 20 s^{-1}. Panel B, the pre-steady-state burst rate determined for each transient by using the burst equation (eq 3) and plotted as a function of [α-^{32}P]MgATP concentration. These data were fit to eq 4 (solid line). The [α-^{32}P]-MgATP concentrations used were sufficiently high such that ATP binding (k_{+1}) was no longer limiting the rate of the first turnover. Therefore, the maximum burst rate determined from eq 4 predicts the maximum rate of hydrolysis, k_{+2} = 93 ± 38 s^{-1}. Panel C, the amplitude of the pre-steady-state burst determined for each transient using the burst equation (eq 3) and plotted as a function of [α-^{32}P]-MgATP concentration. The data were fit to a hyperbola (solid line) with 5.5 ± 0.5 μM as the maximum burst amplitude and $K^{app}_{d,ATP}$ = 87 ± 27 μM. Panels B and C include additional data obtained from experiments not shown in panel A.

Figure 5C, $K^{app}_{d,ATP}$ = 87 ± 27 μM. Therefore, these results using two different methods to analyze the data indicate that ATP binds weakly to the MT·K401 complex (~100 μM), and there is a fast $k_{off,ATP}$ on the order of 100–300 s^{-1}.

In Figure 4A the data were fit by numerical integration to the mechanism in Scheme 1 and the rate constants in the figure legend. The data of each transient in Figure 4A were also fit to the burst equation (eq 3) to determine k_{+1}, k_{-1}, the burst amplitude (A), and the $K^{app}_{d,ATP}$ (Figure 4, parts B and C). Although the computer simulations are more accurate for the final assignment of the rate constants to the mechanism, it is important that the results from the equations be consistent with the rate constants determined by numerical integration (Johnson, 1992). The two independent methods to analyze the data yielded a second-order rate constant for ATP binding, k_{+1} = 0.8–3 μM^{-1} s^{-1}, k_{-1} = 100–300 s^{-1}, and the $K^{app}_{d,ATP} \simeq$ 100 μM.

Time Course of ATP Hydrolysis. Acid-quench experiments were performed as a function of [α-^{32}P]MgATP concentration to determine the rate of ATP hydrolysis (Figure 5). The determination of the hydrolysis step (k_{+2}) requires sufficiently high concentrations of substrate such that ATP binding does not limit the first turnover. Therefore at high ATP concentrations, the first-order rate constant for the pre-steady-state burst is the rate constant k_{+2}, the hydrolysis step. Figure 5A shows the acid-quench transients as a function of ATP concentration. Although the data indicate an increase in the burst rate as a function of ATP concentration, k_{+2} the rate constant for the hydrolysis step is a constant independent of ATP concentration.

The data in Figure 5, parts B and C, were obtained by fitting the data of each transient in Figure 5A to the burst equation (eq 3). Figure 5B shows the plot of the burst rate as a function of [α-^{32}P]MgATP concentration. The fit of the data to eq 4 yields a maximum burst rate of 93 ± 38 s^{-1} which represents k_{+2}. In Figure 5C, the amplitude of the burst was plotted as a function of [α-^{32}P]MgATP concentration. The data were fit to a hyperbola with the maximum burst amplitude = 5.5 ± 0.5 μM and the $K^{app}_{d,ATP}$ = 87 ± 27 μM. Thus, two independent methods to evaluate the data predicted k_{+2} = 70–120 s^{-1}.

Rate-Limiting Product Release. The observation of the pre-steady-state burst in the acid quench transients indicated that product release was rate-limiting for the MT·K401 ATPase. The rate of product release was obtained from the linear phase of the transients in Figures 4 and 5, and this rate constant is presumed to represent rate-limiting ADP release rather than P_i release although this needs to be determined experimentally. The rate of P_i release (k_{+3}) was investigated by the [^{18}O] exchange experiments of Hackney (1988). He reported that the MT·kinesin preparation (native bovine brain) did hydrolyze ATP but with essentially no extra incorporation of water-derived oxygens. Additional experiments indicated that in the absence of microtubules, P_i release is dramatically faster than ADP release, and ADP release in the absence of microtubules is rate-limiting. Hackney's interpretation of his results was that P_i release (k_{+3}) occurs faster than the reversal of the hydrolysis step (k_{-2}) and significantly faster than ADP release (k_{+4}).

Our determination of product release was based on the linear phase of our burst experiments as well as information obtained from the steady-state experiments. The variability in the reported value of k_{cat} = 10–20 s^{-1} is due to differences in individual preparations. For each preparation of K401, steady-state measurements were made to determine the k_{cat} at saturating concentrations of microtubules and MgATP. The k_{cat} determined for steady-state turnover was used in calculations with the rate constants, k_{+2} and k_{+4} according to eq 1:

$$k_{cat} = k_{+2}k_{+4}/(k_{+2} + k_{-2} + k_{+4}) \quad (1)$$

Therefore, the rate constant determined for k_{+4} was consistent with the steady-state kinetics as well as the pre-steady-state kinetics for each K401 preparation.

DISCUSSION

Mechanism of the MT·Kinesin ATPase Pathway. Analysis of the ATP concentration dependence of the pre-steady-state kinetics led to the minimal mechanism of the MT·kinesin pathway of the kinesin ATPase as presented in Scheme 1 with the rate constants in Table 1. This model could not have been determined without the experiments at high ATP concentrations, and these high ATP experiments required high concentrations of enzyme. Thus, the pre-steady-state experiments were facilitated by the cloning of the kinesin heavy chain (Yang *et al.*, 1988, 1989) and the subsequent expression of active motor domains (Gilbert & Johnson, 1993). Fur-

thermore, these truncated kinesin preparations are capable of normal force production because bacterially expressed kinesin polypeptides promote motility at rates that are equivalent to purified native kinesin (Yang *et al.*, 1990; Stewart *et al.*, 1993).

The results presented here have provided new information about kinesin as molecular motor and its interaction with microtubules to generate force for intracellular motility. The pre-steady-state kinetics have shown that MgATP binds weakly to the MT·kinesin complex which is reflected by the $K_{d,ATP}^{app} \simeq 100\ \mu M$. In addition, the kinetic results reveal a fast $k_{off,ATP}$ that results in partitioning of the M·K·ATP complex between ATP hydrolysis (k_{+2}) and ATP release (k_{-1}). The reduced burst amplitude observed is attributed to this fast $k_{off,ATP}$. Furthermore, the observation of the pre-steady-state burst in the acid-quench experiments indicates that the rate-limiting step occurs after ATP hydrolysis. Our results in combination with Hackney's oxygen exchange studies (1988) suggest that it is ADP product release that is rate limiting during steady-state turnover rather than P_i release. Thus, microtubules are acting to increase $k_{off,ADP}$ from 0.01 s^{-1} in the absence of microtubules to 10–20 s^{-1} at saturating microtubules. At this time, we do not have the data to determine if microtubules are also affecting other steps in the pathway. It should be emphasized that the mechanism in Scheme 1 is a minimal mechanism because the rapid quench experiments have not provided evidence in support of additional binding steps or conformational changes. Thus, the model as presented in Scheme 1 with rate constants (Table 1) will be very important in our interpretation of the stopped-flow results that measure protein dynamics of the MT·K401 complex occurring during ATP turnover.

ATP Binding and Hydrolysis by the MT·K401 Complex. The model that we have proposed in Scheme 1 is the simplest model. At low ATP concentrations, the hydrolysis of ATP during the first turnover is limited by ATP binding. As the concentration increases, the rate of ATP binding becomes sufficiently fast such that ATP binding no longer limits the rate of the first turnover, and the maximum rate of hydrolysis can be measured. P_i release occurs rapidly (Hackney, 1988), and it is ADP product release at 10–20 s^{-1} that limits steady-state turnover. The measurement of the $K_{d,ATP}^{app}$ at $\sim 100\ \mu M$ indicates that ATP binds weakly to the MT·K401 complex, and the reduction in burst amplitude is attributed to the fast $k_{off,ATP}$ at 100–300 s^{-1}.

The predictions of the simple model are as follows: (1) $k_{-1} > k_{+2}$ which results in a rapid equilibrium comprised of k_{+1} and k_{-1}. Experimentally, this rapid equilibrium would result in a reduced burst amplitude and a K_d which indicates weak binding of ATP to the MT·K401 complex. The simple model accounts for the observed burst amplitude and K_d. (2) This model also predicts that the hydrolysis transient from the acid-quench experiment would be similar to the ATP binding transient from the pulse–chase experiment because of the fast rate of k_{-1} relative to k_{+2} and the weak binding of ATP to the MT·K401 complex. Thus, there is little accumulation of the K·ATP intermediate that results because of tight ATP binding and is resolved by the pulse–chase experiments. Our data show transients in which ATP binding and hydrolysis are almost superimposed. (3) To a first approximation, the rate constant of the pre-steady-state burst (k_b) is defined as

$$k_b = \frac{K_1 k_{+2}[ATP]}{(K_1[ATP] + 1)}$$

where $K_1 k_{+2}$ is the apparent second-order rate constant for ATP binding. The values calculated for the burst rates (k_b) using $K_1 = 0.01\ \mu M^{-1}$ and $k_{+2} = 100\ s^{-1}$ are comparable with the experimental measurement of the burst rates shown in Figures 4B and 5B. Thus, the data presented lead to the simple model proposed in Scheme 1. The kinetics although are somewhat more complex than can be accounted for by the equation presented above, and these complexities are fully accounted for in the computer simulations (Figures 4A and 5A).

The model in Scheme 1 though proposes simple one-step binding for ATP to the MT·K401 complex. It is somewhat naive to expect single-step substrate binding for the MT·K401 complex with our knowledge of the actomyosin and MT·dynein contractile systems. However, until the stopped-flow experiments are performed and there is evidence for additional steps in the mechanism, the mechanism proposed in Scheme 1 is sufficient to account for the data.

When one evaluates the apparent second-order rate constants for ATP binding, the MT·K401 complex does not appear strikingly different in comparison to actomyosin ($3\ \mu M^{-1}\ s^{-1}$), MT·dynein complex ($4.6\ \mu M^{-1}\ s^{-1}$), or to bovine brain kinesin as the free enzyme ($2.5–6\ \mu M^{-1}\ s^{-1}$). In each case, the apparent second-order rate constant for ATP binding is $\ll 10^9\ M^{-1}\ s^{-1}$, the theoretical bimolecular rate constant for a diffusion-controlled reaction. Yet, the initial evaluation of the MT·K401 pulse–chase experiments to acid-quench experiments were surprising because (1) the transient for ATP hydrolysis was essentially superimposed on the ATP binding transient and (2) a low burst amplitude was observed in the pulse–chase experiments. These results seem to imply that kinesin as a molecular motor is different from myosin and dynein. Yet, what appear to be differences may reflect the techniques used and the presentation of the experimental results. For example, rapid quench experiments at high ATP and microtubule concentrations were not performed for the MT·dynein complex because of difficulty in mixing high concentrations of the MT·dynein complex. Therefore, the quench data for experiments comparable to those shown in Figures 4 and 5 have not been reported. In spite of the complexities and technical difficulties in studying the myosin and dynein ATPases, we have learned that both myosin and dynein bind ATP more tightly as free enzymes than as actomyosin or the MT·dynein complex. In each case, the binding of ATP promotes the very rapid ($>1000\ s^{-1}$) dissociation of E·ATP from F-actin or the microtubule; and hydrolysis occurs after dissociation from the filament. Furthermore, for both the myosin and dynein ATPases, force production is associated with the product release step(s) (Hibberd *et al.*, 1985; Webb *et al.*, 1986; Holzbaur & Johnson, 1989b).

Sadhu and Taylor (1992) have defined the nucleotide binding steps for bovine brain kinesin in the absence of microtubules using fluorescent analogs, mant-ATP and mant-ADP. Their results have defined a two-step mechanism for ATP binding: the initial formation of a collision complex followed by a conformational change. The maximum rate of binding was determined by the conformational change of the kinesin·ATP intermediate at 150–200 s^{-1} for mant-ATP. Similar mechanisms for ATP binding have been demonstrated for myosin and actomyosin (Taylor, 1991; Woodward *et al.*, 1991, and references within each). Our results do not exclude the possibility of a two-step binding mechanism for MT·K401 as discussed above, yet at this time, we do not have data to support any additional steps. Furthermore, our data do not give information about the step at which K401 dissociates from the microtubule, and the mechanism proposed in Scheme

1 is consistent with K401 dissociation from the microtubule prior to or after hydrolysis.

The rate of hydrolysis determined for MT·K401 at saturating ATP and microtubules (70–120 s^{-1}) is comparable to that for the axonemal dynein ATPase (50–150 s^{-1}). Similar rapid quench experiments for the MT·dynein complex were not performed because of the inability to use the high concentrations of the MT·dynein complexes required. However, the light-scattering data of the dynein·ATP dissociation from the MT·dynein complex at >1000 s^{-1} upon addition of ATP indicate that ATP hydrolysis occurs when dynein is off the microtubule. For actomyosin, the rate of ATP hydrolysis occurs at ~150 s^{-1} with S1 from rabbit skeletal myosin. Furthermore, ATP hydrolysis can occur with myosin·ATP dissociated from the actin filament (Lymn & Taylor, 1971) or with myosin·ATP still attached to F-actin [high actin concentrations, low ionic strength (Stein *et al.*, 1979)]. Sadhu and Taylor (1992) also measured the rate of the hydrolysis step for bovine brain kinesin in the absence of microtubules. Their rate constant for the ATP hydrolysis step at 6–8 s^{-1} is significantly smaller than the rate we determined at 70–120 s^{-1}. The initial interpretation of the data is that microtubules are also activating the rate of ATP hydrolysis indicating that the hydrolysis step for the MT·kinesin complex occurs with kinesin still in association with the microtubule. However, such interpretation is premature without the rapid quench experiments for K401 as the free enzyme. First, because of the inability to purify large amounts of native bovine brain kinesin, Sadhu and Taylor (1992) performed their rapid quench experiments at intermediate ATP concentrations; yet because ATP binds tightly to kinesin in the absence of microtubules, the concentrations of ATP used (1.5–10 μM) appear sufficient such that ATP binding was not limiting the first turnover. The main reason to be conservative in the comparison of the results of native kinesin and MT·K401, is the concern about the native kinesin preparation. Hackney *et al.* (1992) have characterized a folded conformation of kinesin in which the tail portion bends back onto the motor head domain. This preparation exhibits reduced rates of ATP turnover even in the presence of microtubules. Therefore, if the kinesin preparation used by Sadu and Taylor did contain a significant proportion of the kinesin in an inhibited form, the k_{+2} determined for the hydrolysis step could be suppressed rather than represent the true chemistry rate for the uninhibited motor domain. The k_{cat} reported for the MT·kinesin complex by Sadhu and Taylor was 3.1 s^{-1} and is reduced relative to the k_{cat} for MT·K401 at 10–20 s^{-1}. The buffer conditions reported by Sadhu and Taylor favor the folded 9S (inhibited) conformation of kinesin. Therefore, the differences in the results may represent differences in the kinesin preparations rather than suggest that microtubules also act at the hydrolysis step to increase the rate of ATP hydrolysis.

Product Release. The observation of a burst in the acid quench experiments indicates that the rate-limiting step in the mechanism occurs after ATP hydrolysis. The rate for product release at 10–20 s^{-1} was obtained from the linear phase of the pre-steady-state kinetics, and this rate was assigned to ADP product release rather than P_i release based in part on the oxygen-exchange studies with the MT·kinesin complex (Hackney, 1988). Furthermore, the observation that K401 is purified with ADP bound at the active site is indicative that K401·ADP is the intermediate that microtubules bind. Therefore, these results indicate that microtubules bind the K401·ADP intermediate and stimulate ADP product release ~1000-fold from 0.01 s^{-1} in the absence of microtubules to 10–20 s^{-1} at saturating microtubule and ATP concentrations. Holzbaur and Johnson (1989a,b) thoroughly characterized product release for axonemal dynein. Their results show that microtubules bind to the dynein·ADP intermediate and increase ADP release from 4 s^{-1} in the absence of microtubules to 50–150 s^{-1} in the presence of microtubules. P_i release is not activated by microtubules as in the case of actomyosin. Furthermore, ADP product release was the step associated with force production for the axonemal dynein–microtubule contractile system.

Motility and Force Production. These mechanistic studies were pursued to understand kinesin-promoted motility and force production. We were prepared to see a distinctly different mechanism for the MT·kinesin ATPase in comparison to actomyosin and MT·dynein ATPases because of recent *in vitro* motility results (Howard *et al.*, 1989; Block *et al.*, 1990; Romberg & Vale, 1993). These studies showed that single kinesin molecules (two heads) promote microtubule-based translocations at rates somewhat faster than multiple motors. Furthermore, kinesin-promoted translocations were for longer distances prior to detachment. These results were in striking contrast to actomyosin. For the actomyosin system, multiple motors are required for movement, and the rates increase as the motor number increases (Uyeda *et al.*, 1991). Although single or a small number of myosin motors will bind F-actin in the absence of nucleotide, addition of ATP results in complete dissociation such that the filament and myosin diffuse away from each other. The interpretation of these motility results was that kinesin unlike myosin spends more of its cycle time in association with the filament with detachment long enough for the necessary conformational change for movement but with a release time brief enough such that there is not time for the microtubule and kinesin to diffuse away from each other. Mechanistic conclusions that attempt to go beyond this simple interpretation cannot be derived from the motility data alone.

For myosin, force is developed by the transition from A·M·ADP·P_i to the high-energy A·M*·ADP·P_i intermediate. P_i is released to form a second force-generating state, A·M*·ADP (Dantzig *et al.*, 1992). For dynein, the high-energy intermediate, D*·ADP, results after P_i release, and this is the intermediate that microtubules bind resulting in MT·D*·ADP. Force (discussed for MT·D) continues to be exerted until the power stroke is complete with the dynein head moving relative to the microtubule lattice. The dynein head does not dissociate from the microtubule until the MT·D complex rebinds ATP (Holzbaur & Johnson, 1989b). This model requires that dynein be more tightly bound to the microtubule in the MT·D*·ADP state than either MT·D·ATP or MT·D·ADP·P_i states and that ATP and ADP be more weakly bound to the MT·dynein complex than to dynein free in solution. The kinetic and thermodynamic results support this model for force production for both actomyosin and MT·dynein. Although we do not have all the information we need to define the complete mechanism for kinesin, the results presented in this paper are consistent with the mechanisms for both myosin and dynein. The MT·K complex binds ATP weakly. ATP hydrolysis occurs either prior to or after dissociation from the microtubule, and P_i release is fast (Hackney, 1988) relative to ADP release. Microtubules rebind to the K·ADP intermediate, and ADP is released from the MT·kinesin complex. What appears unique about kinesin is its very tight binding of ADP in the absence of microtubules. The current data establish that ADP binds weakly to the MT·kinesin complex, and these results are consistent with the

power stroke and force production occurring during ADP release step(s). To understand the single-motor results for kinesin will require that we define the steps and rate constants for kinesin dissociation from and reassociation with the microtubule. The current data indicate that kinesin shows more similarities to the myosin and dynein ATPases than differences. Ultimately, we may find that the mechanistic differences reflect functional differences in the cell as well as the distinct motility requirements of each of these molecular motors.

NOTE ADDED IN PROOF

Mass analysis by scanning transmission electron microscopy has indicated that K401 is a monomer (56 276 ± 19 169 Da, $n = 398$) (Susan P. Gilbert, Kenneth A. Johnson, and Joseph S. Wall, unpublished results).

ACKNOWLEDGMENT

We thank N. R. Lomax, the Drug Synthesis and Chemistry Branch, Division of Cancer Treatment, National Cancer Institute, for providing taxol and Dr. Smita Patel, Ohio State University, and Drs. Taro Fujimori and Ahamindra Jain (Pennsylvania State University) for helpful discussions and critical reading of the manuscript.

REFERENCES

Aizawa, H., Sekine, Y., Takemura, R., Zhang, Z., Nangaku, M., & Hirokawa, N. (1992) *J. Cell Biol. 119*, 1287–1296.

Anderson, K. S., Sikorski, J. A., & Johnson, K. A. (1988) *Biochemistry 27*, 7395–7406.

Barshop, B. A., Wren, R. F., & Frieden, C. (1983) *Anal. Biochem. 130*, 134–145.

Block, S. M., Goldstein, L. S. B., & Schnapp, B. J. (1990) *Nature (London) 348*, 348–352.

Borisy, G. G., Olmsted, J. B., Marcum, J. M., & Allen, C. (1974) *Fed. Proc. 33*, 167–174.

Brady, S. T. (1985) *Nature (London) 317*, 73–75.

Dantzig, J. A., Goldman, Y. E., Millar, N. C., Lacktis, J., & Homsher, E. (1992) *J. Physiol. 451*, 247–278.

Eisenberg, E., & Hill, T. L. (1985) *Science 227*, 999–1006.

Endow, S. A., & Titus, M. A. (1992) *Annu. Rev. Cell Biol. 8*, 29–66.

Geeves, M. A. (1992) *Philos. Trans. R. Soc. London, B 336*, 63–71.

Gho, M., McDonald, K., Ganetzky, B., & Saxton, W. M. (1992) *Science 258*, 313–316.

Gilbert, S. P., & Johnson, K. A. (1993) *Biochemistry 32*, 4677–4684.

Goldman, Y. E. (1987) *Annu. Rev. Physiol. 49*, 637–654.

Goldstein, L. S. B. (1991) *Trends Cell Biol. 1*, 93–98.

Goodson, H. V., & Spudich, J. A. (1993) *Proc. Natl. Acad. Sci. U.S.A. 90*, 659–663.

Hackney, D. D. (1988) *Proc. Natl. Acad. Sci. U.S.A. 85*, 6314–6318.

Hackney, D. D. (1992) *Philos. Trans. R. Soc. London, B 336*, 13–18.

Hackney, D. D., & Clark, P. K. (1984) *Proc. Natl. Acad. Sci. U.S.A. 81*, 5345–5349.

Hackney, D. D., Malik, A.-S., & Wright, K. W. (1989) *J. Biol. Chem. 264*, 15943–15948.

Hackney, D. D., Levitt, J. D., & Wagner, D. D. (1991) *Biochem. Biophys. Res. Commun. 174*, 810–815.

Hackney, D. D., Levitt, J. D., & Suhan, J. (1992) *J. Biol. Chem. 267*, 8696–8701.

Harrison, B. C., Marchese-Ragona, S. P., Gilbert, S. P., Cheng, N., Steven, A. C., & Johnson, K. A. (1993). *Nature (London) 362*, 73–75.

Hibberd, M. G., & Trentham, D. R. (1986) *Annu. Rev. Biophys. Biophys. Chem. 15*, 119–161.

Hibberd, M. G., Dantzig, J. A., Trentham, D. R., & Goldman, Y. E. (1985) *Science 228*, 1317–1319.

Holzbaur, E. L. F., & Johnson, K. A. (1986) *Biochemistry 25*, 428–434.

Holzbaur, E. L. F., & Johnson, K. A. (1989a) *Biochemistry 28*, 5577–5585.

Holzbaur, E. L. F., & Johnson, K. A. (1989b) *Biochemistry 28*, 7010–7016.

Howard, J., Hudspeth, A. J., & Vale, R. D. (1989) *Nature (London) 342*, 154–158.

Johnson, K. A. (1983) *J. Biol. Chem. 258*, 13825–13832.

Johnson, K. A. (1985) *Annu. Rev. Biophys. Biophys. Chem. 14*, 161–188.

Johnson, K. A. (1986) *Methods Enzymol. 134*, 677–705.

Johnson, K. A. (1992) *Enzymes (3rd Ed.)*, 1–61.

Lowry, O. H., Rosebrough, N. J., Farr, A. L., & Randall, R. J. (1951) *J. Biol. Chem. 193*, 265–275.

Lymn, R. W., & Taylor, E. W. (1970) *Biochemistry 9*, 2975–2983.

Lymn, R. W., & Taylor, E. W. (1971) *Biochemistry 10*, 4617–4624.

Omoto, C. K., & Johnson, K. A. (1986) *Biochemistry 25*, 419–427.

Porter, M. E., & Johnson, K. A. (1983) *J. Biol. Chem. 258*, 6582–6587.

Romberg, L., & Vale, R. D. (1993) *Nature (London) 361*, 168–170.

Sadhu, A., & Taylor, E. W. (1992) *J. Biol. Chem. 267*, 11352–11359.

Schacterle, G. R., & Pollack, R. L. (1973) *Anal. Biochem. 51*, 654–655.

Scholey, J. M., Porter, M. E., Grissom, P. M., & McIntosh, J. R. (1985) *Nature (London) 318*, 483–486.

Shelanski, M. L., Gaskin, F., & Cantor, C. R. (1973) *Proc. Natl. Acad. Sci. U.S.A. 70*, 765–768.

Skoufias, D. A., & Scholey, J. M. (1993) *Curr. Opin. Cell Biol. 5*, 95–104.

Sleep, J. A., & Boyer, P. D. (1978) *Biochemistry 17*, 5417–5422.

Sleep, J. A., & Hutton, R. L. (1980) *Biochemistry 19*, 1276–1283.

Sloboda, R. D., Dentler, W. L., & Rosenbaum, J. L. (1976) *Biochemistry 15*, 4497–4505.

Stein, L. A., Schwarz, Jr., R. P., Chock, P. B., & Eisenberg, E. (1979) *Biochemistry 18*, 3895–3909.

Stewart, R. J., Pesavento, P. A., Woerpel, D. N., & Goldstein, L. S. B. (1991) *Proc. Natl. Acad. Sci. U.S.A. 88*, 8470–8474.

Stewart, R. J., Thaler, J. P., & Goldstein, L. S. B. (1993) *Proc. Natl. Acad. Sci. U.S.A. 90*, 5209–5213.

Taylor, E. W. (1991) *J. Biol. Chem. 266*, 294–302.

Taylor, E. W. (1992) in *The Heart and Cardiovascular System* (Fozzard, H. A., *et al.*, Eds.) 2nd ed., pp 1281–1293, Raven Press, Ltd., New York.

Trentham, D. R., Bardsley, R. G., Eccleston, J. F., & Weeds, A. G. (1972) *Biochem. J. 126*, 635–644.

Uyeda, T. Q. P., Warrick, H. M., Kron, S. J., & Spudich, J. A. (1991) *Nature (London) 352*, 307–311.

Vale, R. D. (1987) *Annu. Rev. Cell Biol. 3*, 347–378.

Vale, R. D., Reese, T. S., & Sheetz, M. P. (1985) *Cell 42*, 39–50.

Warner, F. D., & McIntosh, J. R. (1989) *Cell Movement*, Vol. 2, Alan R. Liss, Inc., New York, NY.

Webb, M. R., Hibberd, M. G., Goldman, Y. E., & Trentham, D. R. (1986) *J. Biol. Chem. 261* 15557–15564.

Woodward, S. K. A., Eccleston, J. F., & Geeves, M. A. (1991) *Biochemistry 30*, 422–430.

Yang, J. T., Saxton, W. M., & Goldstein, L. S. B. (1988) *Proc. Natl. Acad. Sci. U.S.A. 85*, 1864–1868.

Yang, J. T., Laymon, R. A., & Goldstein, L. S. B. (1989) *Cell 56*, 879–889.

Yang, J. T., Saxton, W. M., Stewart, R. J., Raff, E. C., & Goldstein, L. S. B. (1990) *Science 249*, 42–47.